Raman Imaging The Spatial Distribution And Microstructure Of Insoluble Organic Matter In Carbonaceous Meteorites. R. S. Jakubek[1] and M. D. Fries[2], [1]Jacobs, NASA Johnson Space Center, Houston, TX, USA, [2]NASA Astromaterials Acquisition and
Curation Office, NASA Johnson Space Center, Houston, Texas, USA.

Introduction: Carbonaceous and ordinary chondritic meteorites can contain up to ~5% carbon and host a wide diversity of organic compounds.[1] Meteoritic carbon is a subject of great interest with important implications to solar system formation and the origin of life.[1] Generally, meteoritic carbon is first extracted from the meteorite before study. To do this, a series of solvents will be used to dissolve some of the organic material and the organics in solution can be studied using various techniques.[2] However, less than half (~20-40%) of the organics present are in the soluble fraction. The remaining insoluble organic matter (IOM) is generally extracted by dissolving the surrounding minerals to isolate the organic component and are studies using techniques such as NMR, Raman, and pyrolysis.[3] While these analysis techniques have provided a plethora of valuable information on the organic species in meteorites, the extraction of organics from the meteorite destroys their spatial relationships and mineral associations before analysis.

Raman spectroscopy is a powerful tool for the analysis of carbon in meteorites. For example, Raman of meteoritic carbon is commonly used for the examination of thermal alteration.[4] Raman spectra of meteoritic carbon only show the insoluble fraction because of its strong resonance enhancement[5] while the soluble fraction is unobserved because the concentration of any single molecular species of the organic fraction is small. However, Raman spectroscopy can provide much information on the structure of the IOM, which is generally difficult to study because of its insoluble, non-crystalline nature.

Raman imaging allows for the examination and detailed analysis of molecular and crystalline species across the surface of a sample. In Raman imaging, the sample is rastered under the objective of a Raman microscope and individual Raman spectra are collected at different points on the sample surface. Collecting a 2D array of Raman spectra produces a Raman image

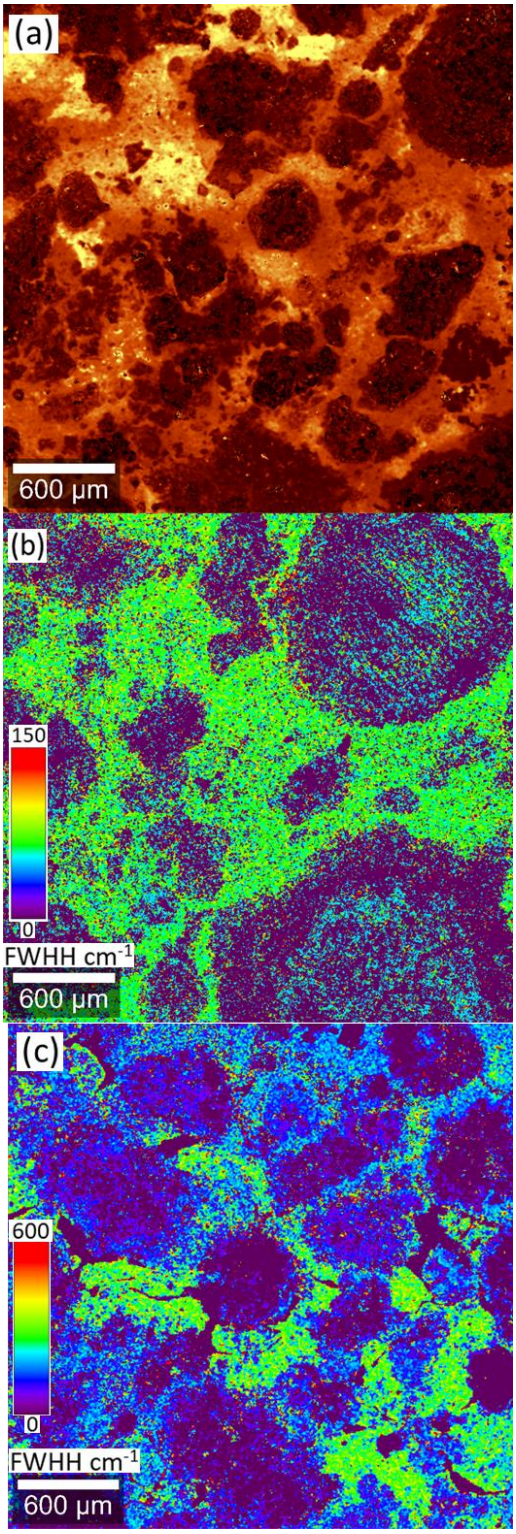

Figure 1 (At right): (a) Raman image of IOM in RBT 04133 (CV3) the pixel brightness indicated the intensity of the G and D bands. (b) D band FWHH in MIL 07002 (CV3) showing variation between matrix and chondrule carbon microstructure, and (c) D band FWHH in GRA 06100 (CR2) showing inhomogeneity of carbon structure in the matrix (green vs. blue).

where each pixel in the image is a Raman spectrum. Raman imaging allows for the spatial mapping of meteorite IOM, providing the ability to examine the mineral associations and spatial relationship of IOM structure.

In this work we collect large, 3x3mm Raman images of different carbonaceous chondrites. We discuss the IOM structural heterogeneity and its spatial distribution observed in the Raman images, which have implications on the meteorite's formation and thermal alteration histories.

Methods: Raman images were collected using a WITec alpha300R Raman microscope using 488 nm excitation focused to a 3um beam size using a 20x objective. An incident laser power of 40uW was measured at the sample surface. For each Raman image, a 600x600 array of Raman spectra were collected over a 3x3mm area on each sample surface producing a total of 360,000 Raman spectra at a spatial resolution of 5um. The single Raman spectrum accumulation time used was 1s resulting in a Raman image collection time of ~100 hours.

Raman images were collected on thin section on loan from the Antarctic meteorite collection at JSC. The meteorites examined in this study are Allan Hills (ALH) 77003,101 (CO3.6), ALH 84029,7 (CM2), Buckley Island (BUC) 10933,10 (CR2), Dominion Range (DOM) 08004,5 (CO3), Elephant Moraine (EET) 96029,8 (CM2), EET 99430,5 (CK4), Graves Nunataks (GRA) 06100,41 (CR2), Grosvenor Mountains (GRO) 17063,6 (CR2), Lonewolf Nunataks (LON) 94101,13 (CM2), Meteorite Hills (MET) 01079,11 (CM1), Miller Range (MIL) 07002,15 (CV3), MIL 090010,39 (CO3), Roberts Massif (RBT) 04133,11 (CV3), and Dar al Gani (DAG) 749 (CO3).

Results: The Raman spectra of IOM vary between meteorites revealing the structural difference between the IOM. As previously demonstrated [4], the lower thermally altered meteorites show IOM Raman spectra with broad G and D bands and a low intensity D band relative to the G band (low, I_D/I_G) consistent with more disordered IOM compared to more thermally altered meteorites. In addition, the IOM spectral and structural differences across meteorite types follows the general trends as previously described.[3]

In addition, we observe structural heterogeneity of the IOM within single Raman images and the IOM structures are spatially zoned. A common observation is that the IOM in the matrix is structurally different compared to that found in the chondrules. Figure 1b and c demonstrate this by showing the change in the D band FWHH, a marker for IOM disorder and thermal alteration[4], at different locations within the sample. For brevity we will just discuss the results for one sample here. Figure 1b shows a MIL 07002,15 Raman image of the FWHH of the IOM D band, which along with I_D/I_G is generally an indicator of thermal maturity of IOM and thus the petrologic type of the meteorite.[4] However, as observed in figure 1b, the meteorite contains 3 distinct IOM structures that are spatially sorted. The matrix contains IOM with a D band width of 70 cm^{-1} and an I_D/I_G ratio of ~1.2 (shown as green pixels in figure 1b). In contrast, the chondrules contain 2 different populations of IOM, the bulk of the chondrule IOM contains a D band width of 63 cm^{-1}, slightly more narrow than that of the matrix (shown as blue pixels in figure 1b). In addition, there is a small population of IOM within the chondrule that contains a significantly broader D band width of 121 cm^{-1} (shown as red pixels in figure 1b). Both IOM species within the chondrule contain a I_D/I_G ratio of ~1.0, significantly lower compared to the matrix. If it is assumed that the differences in IOM structure derive entirely from thermal alteration, these differences reflect different peak thermal alteration temperatures reached by different components of the meteorite. For MIL 07002,15 the IOM spectral differences would indicate that the matrix experienced higher peak thermal alteration temperatures compared to the chondrules.

The observation of less thermally altered IOM within chondrules is a surprising result that implies a thermal history where the matrix was heated separately and to a greater extent from the chondrule before parent body formation. This result contradicts the general assumption that chondrules experienced greater thermal excursions than either the matrix or coalesced parent body, which would lead to chondrule MMC with generally greater ordering than that seen in the matrix. This result, along with that of the other images collected in this work, highlights that much work needs to be done examining the spatial distribution of carbon in carbon-bearing meteorites

Acknowledgments: Funding for this work was provided as an Advanced Curation project run by the NASA Astromaterials Acquisition and Curation Office, Johnson Space Center.

References: [1] Pizzarello, S., Shock, E. (2010). *Cold Spring Harbor Perspectives in Biology*, 2(3), a002105. [2] Pizzarello, S., & Cooper, G. W. (2001). *MAPS*, 36(7), 897-909. [3] Busemann, H., Alexander, M. O. D., & Nittler, L. R. (2007). *MAPS*, 42(7-8), 1387-1416. [4] Bonal, L., Quirico, E., Flandinet, L., & Montagnac, G. (2016). *GCA*, 189, 312-337. [5] Ferrari, A. C., & Robertson, J. (2001). *Phys.Rev.B*, 64(7), 075414.